



Discovery of *N*-(3-bromo-1*H*-indol-5-yl)-quinazolin-4-amine as an effective molecular skeleton to develop reversible/irreversible pan-HER inhibitors



Qidong Tang^{a,1}, Ting Peng^{b,1}, Jie Hu^{a,1}, Tao Zhang^{b,1}, Pengqin Chen^{a,c}, Daoxing Chen^a, Yunjie Wang^a, Lingfeng Chen^d, Linjiang Tong^b, Yi Chen^b, Hua Xie^{b,e,**}, Guang Liang^{a,c,d,*}

^a Chemical Biology Research Center, School of Pharmaceutical Sciences, Wenzhou Medical University, Wenzhou, 325035, China

^b Division of Anti-Tumor Pharmacology, State Key Laboratory of Drug Research, Shanghai Institute of Materia Medica, Chinese Academy of Sciences, Shanghai, 201203, China

^c Wenzhou Institute, University of Chinese Academy of Sciences, Wenzhou, 325001, China

^d School of Pharmacy, Hangzhou Medical College, Hangzhou, 311399, China

^e Zhongshan Institute for Drug Discovery, Shanghai Institute of Materia Medica, Chinese Academy of Sciences, Zhongshan, 528400, China

ARTICLE INFO

Article history:

Received 31 December 2021

Received in revised form

26 February 2022

Accepted 28 February 2022

Available online 2 March 2022

Keywords:

Reversible/irreversible pan-HER inhibitor

Quinazolin-4-amine derivatives

Anti-tumor

Structure-activity relationship

ABSTRACT

Pan-HER inhibitors exhibit extensive biological activity and offer unique advantages and usually bind to targets in an irreversible manner. Owing to the off-target toxicity of irreversible inhibitors, reversible pan-HER inhibitors are desirable. Herein, we describe the process of *N*-(ring structure fused phenyl) quinazolin-4-amine-based design, synthesis, and biological evaluation of pan-HER inhibitors *in vitro* and *in vivo*. Compound **C5**, with the molecular skeleton of *N*-(3-bromo-1*H*-indol-5-yl)-quinazolin-4-amine, displayed irreversible binding just like other effective pan-HER inhibitors. To our surprise, compound **C6**, which possessed the same skeleton, was found to be a high-strength reversible pan-HER inhibitor. This compound was capable of inhibiting HER1s (such as EGFR T790M/L858R and WT), HER2, and HER4 and can be considered as a breakthrough in the development of pan-HER inhibitors. Altogether, *N*-(3-bromo-1*H*-indol-5-yl)-quinazolin-4-amine can serve as an effective molecular skeleton for developing both reversible and irreversible pan-HER inhibitors in the following discovery of antitumor drugs.

© 2022 Elsevier Masson SAS. All rights reserved.

1. Introduction

Human epidermal growth factor receptor (HER, also called EGFR or ErbB) is one of the most extensively studied receptor tyrosine kinases (RTKs) and includes HER1, HER2, HER3, and HER4 [1]. At present, EGFR inhibitors are widely employed for treating non-small cell lung cancer (NSCLC) [2]. However, their effectiveness is

short-lived owing to secondary mutations causing drug resistance. Furthermore, the blocking of EGFR has no effect on HER2 (which behaves as a signal transducer and activator of transcription 3 (STAT3) co-activator for cyclin D1 promoter activation and promotes tumor proliferation), Janus kinase (JAK)/STAT, and HER4 pathways, in which the activation of STAT3 is correlated with tumor growth and malignancy. Regarding the clinical restriction of EGFR TKIs, pan-HER inhibitors have attracted substantial attention. These inhibitors have been effectively employed in treating various cancers, such as breast cancer and NSCLC. Moreover, other cancers, such as gastric, neck, colorectal, and brain cancer, which are strongly related to the over-activity of HER pathways, can also be managed with this category of drugs [3].

Pan-HER inhibitors exhibit extensive biological activities and offer unique advantages, which led to the marketing of afatinib (**1**, Fig. 1, BIBW2992), dacomitinib (**2**), neratinib (**4**), and pyrotinib (**5**)

* Corresponding author. Chemical Biology Research Center, School of Pharmaceutical Sciences, Wenzhou Medical University, Wenzhou, 325035, China.

** Corresponding author. Division of Anti-Tumor Pharmacology, State Key Laboratory of Drug Research, Shanghai Institute of Materia Medica, Chinese Academy of Sciences, Shanghai, 201203, China.

E-mail addresses: hxie@simmm.ac.cn (H. Xie), wzmclianguang@163.com (G. Liang).

¹ These authors contribute equally to this work.

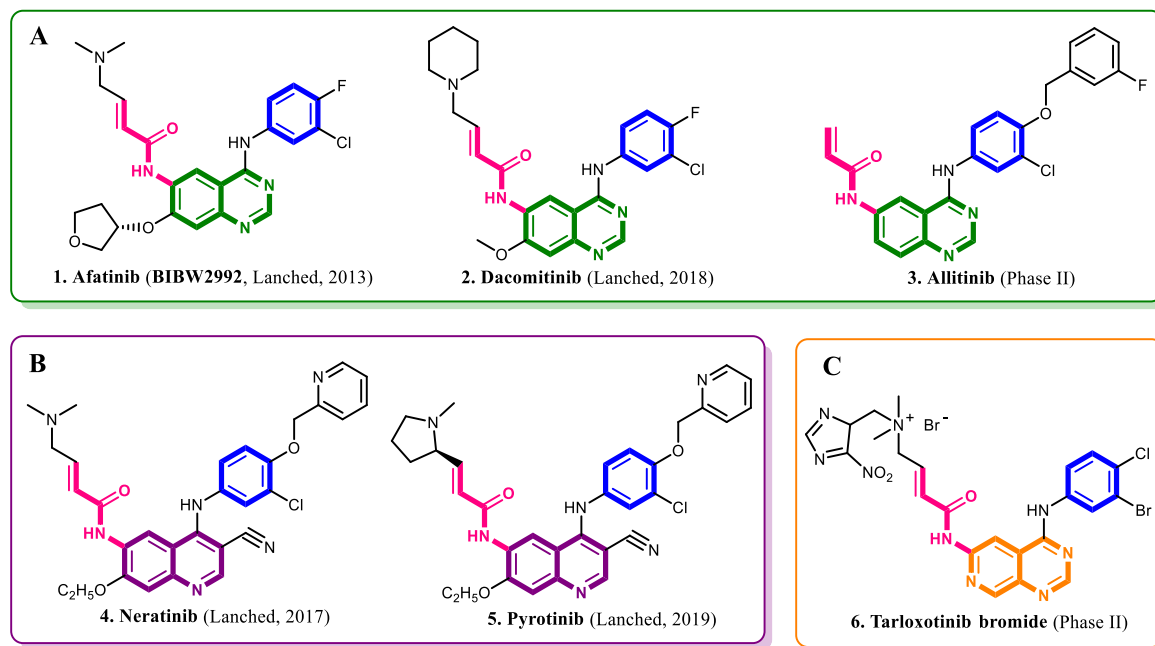


Fig. 1. Three types of marketed or in clinical trials small molecular pan-HER inhibitors. Representative pan-HER inhibitors in the type of quinazoline (A), quinoline (B), and pyrido [3,4-*d*]pyrimidine (C).

in 2013, 2018, 2017, and 2019, respectively [4–6]. These drugs are capable of extensively inhibiting all cancer-related HER-family homodimers and heterodimers and possibly ameliorate the effectiveness and restrict the alternative signaling from receptor cross-talk [3]. BIBW2992 (henceforth used to represent afatinib) has achieved great success in the treatment of NSCLC with exon 21 (L858R) substitution mutations or EGFR exon 19 deletions and is the only drug approved for G719X, S768L, and L861Q mutations [7]. In addition, BIBW2992 could impede the growth and metastasis of pancreatic cancer stem cells via the EGFR/ERK/FOXA2/SOX9 axis [8]. Dacomitinib is used in treating NSCLC and phase II study for neck and brain cancer is ongoing, which could enable patients with NSCLC have longer progression-free and overall survival than with the use of other major EGFR inhibitors [9,10]. Surprisingly, dacomitinib is effective in treating pulmonary hypertension and pulmonary vascular remodeling, whereas gefitinib, lapatinib, and erlotinib do not exhibit any effective therapeutic benefits in both instances [11,12]. Therefore, it is desirable to develop pan-HER inhibitors that are more efficient than the presently available ones.

Till date, the molecular skeletons of pan-HER inhibitors are limited. To the best of our knowledge, pan-HER inhibitors including these four marketed and seven in clinical trials (allitinib (3) [13], tarloxotinib (6) [14], poziotinib [15], canertinib [16], varlitinib [17], pelitinib [18], and sapitinib [19]) could be categorized into three types based on the middle part in their structures (quinazoline, quinoline, and pyrido [3,4-*d*]pyrimidine), as presented in Fig. 1. The fourth positions of these three aromatic heterocyclic rings are all substituted phenyls. Hence, these pan-HER inhibitors only have the molecular skeleton of 4-phenyl-amino-quinazoline (quinoline or pyrido [3,4-*d*]pyrimidine) [20].

Another commonality is that these inhibitors contain the α,β -unsaturated carbonyl group (in the sixth position of quinazoline, quinoline, or pyrido [3,4-*d*]pyrimidine) and undergo Michael reaction, which allows nucleophile introduction (sulfhydryl (-SH) on C797 of HER1) to the double-bond, thus forming covalent Michael adducts [4]. However, the potential for off-target toxicity of irreversible inhibitors via nonspecific binding of the chemically

reactive α,β -unsaturated carbonyl group to the sulfhydryl group in the human body poses immense limitations in their usage. Adverse effects, such as diarrhea, are frequently observed [21], and none of these pan-HER inhibitors could bind to EGFR T790M/L858R in noncovalent form. Therefore, it is of great significance to identify effective reversible pan-HER inhibitors.

Our design inspiration for pan-HER inhibitors came from the crystal structure of BIBW2992 bound to the EGFR complex (PDB ID: 4G5J) [22]. As shown in Fig. 2A, BIBW2992 was located deep in the EGFR protein cavity, and the 3-chloro-4-fluorophenyl group in the 4-position of the quinazoline ring faced THR790 and extended into the hydrophobic pocket. By carefully observing the binding site, we found that there was a large space around the 3-chloro-4-fluorophenyl group. A similar situation could also be seen in the binding interaction of allitinib (AST1306) with the EGFR protein (Fig. 2B), which was investigated in our previous study [23]. Therefore, we attempted to explore whether fusing a five-membered or six-membered ring or a bulkier group with the phenyl ring to form the structures of indole, 1*H*-indazole, quinoline, naphthalene ring, etc., would improve the binding potency with the EGFR protein. Therefore, the molecular skeleton of *N*-(ring structure fused phenyl)quinazoline-4-amine was constructed (Fig. 2C). Herein, we report the *N*-(ring structure fused phenyl)quinazoline-4-amine-based design, synthesis, and biological evaluation for the discovery of both reversible and irreversible pan-HER inhibitors capable of inhibiting HER1s (such as T790M/L858R and wild type (WT)), HER2 and HER4 *in vitro* and *in vivo*.

2. Results & discussion

2.1. Chemistry

The route for synthesizing compounds **A1–12** is listed in Scheme 1. Briefly, the condensation of 2-amino-5-nitrobenzonitrile with *N,N*-dimethylformamide dimethyl acetal (DMF-DMA) produced intermediate **8** [24]. Cyclization of intermediate **8** with a set of prepared heteroaryl amines in the presence of acetic acid (AcOH)

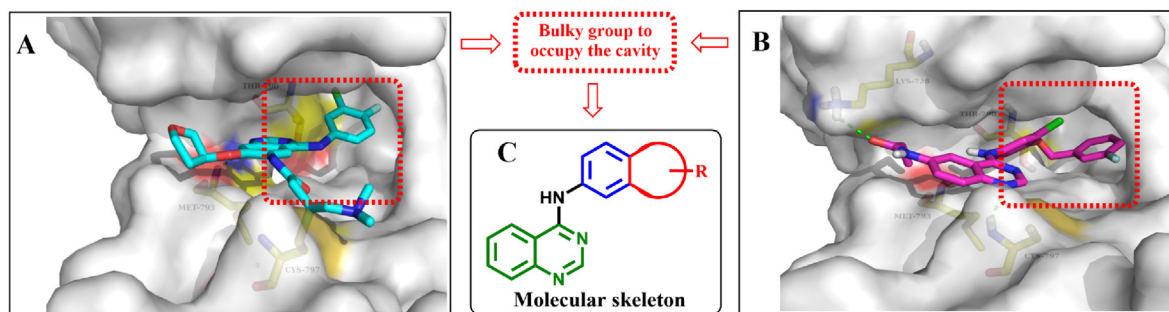
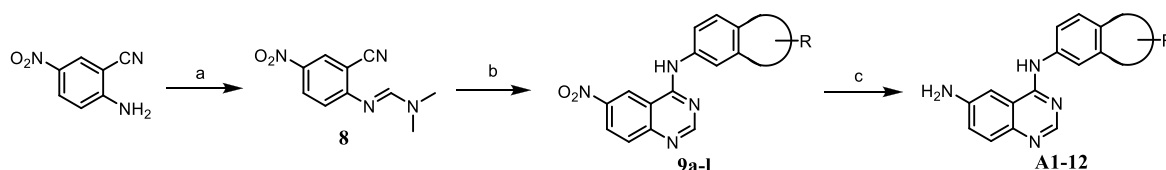


Fig. 2. The design strategy of the molecular skeleton based on *N*-(ring structure fused phenyl)quinazoline-4-amine. (A) Crystal structure of BIBW2992 binding to EGFR. (B) Molecular docking analysis of allitinib binding interaction with EGFR. (C) Molecular skeleton for the target compounds. (PDB ID: 4G5J).



Scheme 1. Synthesis of compounds **A1–12**. Reagents and Circumstances: (a) DMF-DMA, toluene, 115 °C, 2 h, 90%; (b) Corresponding heteroaryl amines, AcOH, 115 °C, 3–6 h, 80–97%; (c) Fe, AcOH, aqueous ethanol (EtOH, 70%), 85 °C, 1 h, 20–76%.

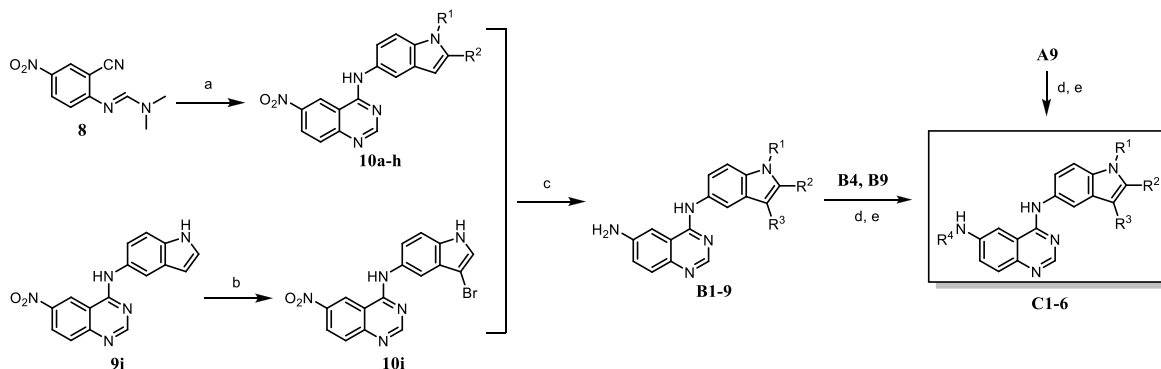
yielded *N*-(substituted-phenyl)-6-nitroquinazolin-4-amines **9a–l** [24]. Reduction of nitro groups of **9a–l** using iron (Fe) powder and AcOH yielded compounds *N*⁴-(substituted-phenyl)quinazoline-4,6-diamines **A1–12** [25].

Scheme 2 depicts the synthetic routes of compounds **B1–9** and **C1–6**. *N*-(1,2-disubstituted-1*H*-indol-5-yl)-6-nitroquinazolin-4-amines **10a–h** were synthesized from intermediate **8** through a reaction with the corresponding substituted-1*H*-indol-5-amines using AcOH as the solvent. 4-(3-bromo-1*H*-indol-5-yl)amino-6-nitroquinazoline **10i** was synthesized via bromination of the intermediate **9i** with *N*-bromosuccinimide (NBS). Reduction of the nitro groups of **10a–i** with iron powder and acetic acid yielded the compounds *N*⁴-(1,2,3-trisubstituted-1*H*-indol-5-yl)quinazoline-4,6-diamines **B1–9** [25]. Finally, **A9**, **B4**, and **B9** were condensed with acryloyl chloride/3-chloropropanoyl chloride to produce the corresponding target compounds **C1–6**.

2.2. Structure-activity relationships (SARs)

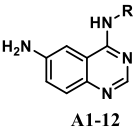
Based on the abovementioned drug design strategy, we first attempted to fuse a five-membered ring, six-membered ring, or

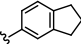
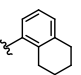
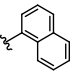
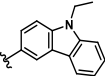
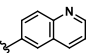
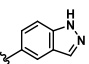
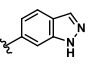
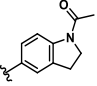
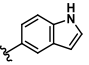
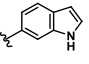
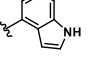
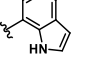
even a bulkier group to the phenylamine group present in the 4-position of quinazoline to form the structures of indole, 1*H*-indazole, quinoline, naphthalene, etc. Second, because all the pan-HER inhibitors mentioned above contain a substituted amino group in the 6-position of quinazoline, the amino group was introduced to the 6-position of the molecular skeleton *N*-(ring structure fused phenyl)quinazoline-4-amine. Correspondingly, a series of compounds (**A1–12**) was synthesized, and the effects of the ring structure fused phenyl groups in the 4-position of quinazoline were examined via kinase activity test against EGFR WT *in vitro* (Table 1) using the enzyme-linked immunosorbent assay (ELISA) [26]. As can be seen from Table 1, compounds with a single five- or six-membered ring fused not only with the 2-position and 3-position (compounds **A2**, **A3**, and **A12**) but also with the 3-position and 4-position (compounds **A1**, **A5**, **A6**, **A9**, and **A10**) of the phenylamino group inhibited EGFR WT to a certain degree. However, bulkier structures fused with the phenylamino group reduced the inhibition (compounds **A4** and **A8**). Interestingly, compound **A9** containing pyrrole fused with the 3-position and 4-position of the phenylamino group (1*H*-indol-5-amine) demonstrated the strongest inhibition, with an IC₅₀ value of 0.65 nM against EGFR WT. On



Scheme 2. Synthesis of compounds **B1–9** and **C1–6**. Reagents and conditions: (a) Corresponding substituted-1*H*-indol-5-amines, AcOH, 115 °C, 3–6 h, 80–97%; (b) NBS, benzoyl peroxide, *N,N*-dimethylformamide (DMF), –10 °C, 15 h, 52%; (c) Fe, AcOH, aqueous EtOH (70%), 85 °C, 1 h, 26–74%; (d) Acryloyl chloride/3-chloropropanoyl chloride, tetrahydrofuran (THF), trimethylamine (TEA), 0 °C, 2 h; (e) Sodium bicarbonate (NaHCO₃), 0 °C, 12 h, 22–52%.

Table 1
Structure and EGFR WT kinase assay of compounds **A1–12**.



Comp.	R	EGFR WT kinase assay IC ₅₀ (nM)
A1		251.3
A2		164.8
A3		1.60
A4		>10000
A5		215.1
A6		2.98
A7		>1000
A8		>10000
A9		0.65
A10		183.7
A11		>1000
A12		25.17

the other hand, changing the position of the nitrogen atom in pyrrole ring (compound **A9** vs compound **A10**) or increasing the number of nitrogen atom to form the pyrazole ring (compound **A9** vs compound **A6**, compound **A10** vs compound **A7**) decreased the potency. These results indicate that 1*H*-indol-5-amine in compound **A9** is the preferred group for potency.

Given that compound **A9** could effectively inhibit EGFR WT, the inhibitory activity on HCC827 cell line (harboring L858R mutation) and H1975 cell line (harboring T790M/L858R mutation) was screened to evaluate the antiproliferative potency using the sulforhodamine B (SRB) colorimetric assessment. The results were unsatisfactory, and the IC₅₀ value against H1975 was 27.22 μM (Table 2). Accordingly, optimization of the substituents in the 1-/2-/3-position of the indole ring of compound **A9** was attempted, and compounds **B1–9** were obtained in the following SARs studies. First, when methyl, propyl, allyl, 3-chloro-benzyl (3-Cl-PhCH₂-), or

3-fluoro-benzyl (3-F-PhCH₂-) groups was introduced to the 1-position of the indole ring of compound **A9**, the potencies against EGFR WT and HCC827 were decreased, whereas that against H1975 were increased (Table 2, compounds **B1–5**). Comparatively, compound **B4** showed relatively potent activity (EGFR WT IC₅₀ = 3.01 nM, HCC827 IC₅₀ = 1.53 μM, H1975 IC₅₀ = 9.82 μM) in compounds **B1–5**. Second, introducing substituents to the 2-position of the indole ring unfavorably affected the inhibitory activity (Table 2, compounds **B6–8**), especially for the activity on EGFR WT compared with compound **A9**. Surprisingly, when bromine atom was introduced to the 3-position to get compound **B9**, the potency on EGFR WT was retained (Table 2, EGFR WT IC₅₀ = 0.74 nM). The IC₅₀ values on HCC827 and H1975 cell lines were increased to 0.03 and 5.90 μM, respectively, which were six and five times more active than that of compound **A9**.

Having obtained these results, we next focused on the modification of compounds **A9**, **B4**, and **B9**, which demonstrated relatively good activity. As shown in Table 3, acryloyl (-COCH=CH₂) and 3-chloropropanoyl (-CO(CH₂)₂Cl) groups were introduced to the amino group of the quinazolinone ring in the active compounds **A9**, **B4**, and **B9** to get the corresponding compounds **C1–2**, **C3–4**, and **C5–6**, respectively. As shown in Table 3, all the compounds **C1–6** exhibited potent inhibition of EGFR WT and T790M/L858R. Especially for the compounds **C5/C6**, the activity reached the nM level, with IC₅₀ values of 0.38/0.72 nM and 2.2/8.2 nM against EGFR WT and T790M/L858R, respectively, which were either superior or comparable to that of BIBW2992 (EGFR WT IC₅₀: 0.67 nM, EGFR T790M/L858R IC₅₀: 3.7 nM). Regarding the activity against EGFR WT, compounds **C5/C6** demonstrated better inhibitory activity than **A1–12** and **B1–9**, except for the fact that the activity of **C6** (EGFR WT IC₅₀: 0.72 nM) was comparable to that of **A9** (EGFR WT IC₅₀: 0.65 nM).

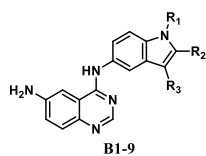
2.3. Inhibitory effect on the phosphorylation of EGFR and the downstream proteins Akt and Erk

The potent EGFR kinase inhibition was further confirmed by examining the inhibitory effects of **C5** and **C6** on EGFR phosphorylation via western blot analysis, such as EGFR WT and T790M/L858R, and downstream protein kinase B (Akt) and extracellular regulated protein kinases (Erk) across A431 (Fig. 3A) and H1975 (Fig. 3B) cells. The results indicated that **C5** and **C6** could effectively inhibit the phosphorylation of EGFR even at a concentration of 1 nM, which was either comparable or superior to that of BIBW2992 in the two cell lines. To our surprise, the inhibitory effect of **C6** was better than that of **C5**. Moreover, **C5** and **C6** could effectively inhibit the phosphorylation of the downstream signaling proteins Erk and Akt at concentrations of 1, 10, 100, or 1000 nM. In addition, **C5** and **C6** could effectively inhibit EGFR, Akt, and Erk phosphorylation in NIH3T3-EGFR WT, L858R, 19D/T790M, T790M/L858R, and insNPG cells at concentrations of 1, 10, or 100 nM, as shown in Fig. S1.

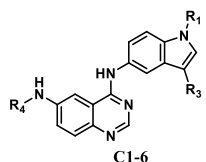
2.4. Pan-HER inhibitor confirmation

To examine the selectivity of **C5** and **C6** on EGFR over other kinases, multi-kinase assay was performed against 13 other tyrosine kinases using ELISA (Table 4). As inferred from the table, **C5** and **C6** exhibited strong inhibitory activities against HER2 (IC₅₀ = 3.5/75.1 nM) and HER4 (IC₅₀ = 1.6/2.0 nM). However, the other 11 RTKs, such as Src, VEGFR2, and EPH-A2, were only weakly inhibited, and all the IC₅₀ values were >10000 nM. Therefore, **C5** and **C6** showed potent selectivity on HER family members.

As the multi-kinase assay revealed that **C5** and **C6** belonged to pan-HER inhibitors, their antiproliferative activity was assessed on

Table 2Structure of compounds **B1–9**, the corresponding kinase activity on EGFR WT and antiproliferative activity on HCC827/H1975 cell lines.

Comp.	R ₁	R ₂	R ₃	EGFR WT kinase assay IC ₅₀ (nM)	HCC827 cell line (L858R) IC ₅₀ (μM)	H1975 cell line (T790M/L858R) IC ₅₀ (μM)
B1	Me	H	H	4020	3.62 ± 0.62	13.89 ± 1.64
B2	propyl	H	H	358.3	7.26 ± 2.16	18.13 ± 0.55
B3	allyl	H	H	351.9	7.73 ± 2.81	16.88 ± 2.07
B4	3-F-PhCH ₂	H	H	3.01	1.53 ± 0.26	9.82 ± 0.85
B5	3-Cl-PhCH ₂	H	H	8.38	1.93 ± 0.36	10.85 ± 0.98
B6	H	Me	H	255.0	5.17 ± 2.27	22.59 ± 5.6
B7	H	C(CH ₃) ₃	H	>1000	13.25 ± 1.66	3.50 ± 0.49
B8	H	COOEt	H	>1000	22.24 ± 1.47	15.02 ± 0.96
B9	H	H	Br	0.74	0.03 ± 0.002	5.90 ± 1.24
A9				0.65	0.18 ± 0.02	27.22 ± 7.18

Table 3Structure and activity on EGFR WT and T790M/L858R of compounds **C1–6**.

Comp.	R ₁	R ₃	R ₄	Kinase assay IC ₅₀ (nM)	
				WT	T790M/L858R
C1	H	H	COCH ₂ =CH ₂	13.7 ± 5.8	13.7 ± 4.3
C2	H	H	CO(CH ₂) ₃ Cl	5.8 ± 1.5	12.6 ± 6.8
C3	3-F-PhCH ₂	H	COCH ₂ =CH ₂	1.1 ± 0.4	1.4 ± 0.7
C4	3-F-PhCH ₂	H	CO(CH ₂) ₃ Cl	6.9 ± 0.7	6.0 ± 2.4
C5	H	Br	COCH ₂ =CH ₂	0.38 ± 0.05	2.2 ± 1.1
C6	H	Br	CO(CH ₂) ₂ Cl	0.72 ± 0.11	8.2 ± 1.2
BIBW2992				0.67 ± 0.08	3.7 ± 1.2

cell lines with high expression of EGFRs/HER2 and low expression of HERs using the SRB colorimetric assay. The data suggested that **C5** and **C6** strongly inhibited the cells with high expression of EGFRs, namely, A431, H1975, and HCC827, and those with high

expression of HER2, namely, SK-BR-3 and BT-474 (Fig. 4). On the contrary, the inhibitory effect was weak on cells with low expression of HERs, i.e., T47D, MCF-7, and SW620.

Encouraged by the results of multi-kinase and antiproliferative assay, we further examined the inhibitory effects of **C5** and **C6** on the phosphorylation of HER2 and the downstream proteins Akt and Erk via western blot analysis. The results signified that these two compounds could effectively inhibit the phosphorylation of HER2 as well as the related downstream proteins including Akt and Erk in the SKOV3 (Fig. 5A) and BT-474 cells (Fig. 5B) at a concentration of 1 or 10 nM in a dose-dependent manner. The trend was similar to that of BIBW2992 in these two cell lines. From these results, we can conclude that **C5** and **C6** belong to the family of pan-HER inhibitors.

2.5. Apoptosis assay

To further reveal the mechanism of cell apoptosis induced by **C5** and **C6**, Annexin V/PI staining was performed. The apoptosis of H1975 cancer cells was detected to study the mechanism of the antiproliferative effect of **C5** and **C6** using flow cytometry. With the aid of the annexin V-FITC and propidium iodide (PI) assay, quantitative analysis of death cells, late-apoptotic cells, and early-apoptotic cells was performed.

Compounds **C5** and **C6**, at concentrations of 0.1, 1 or, 10 μM, were

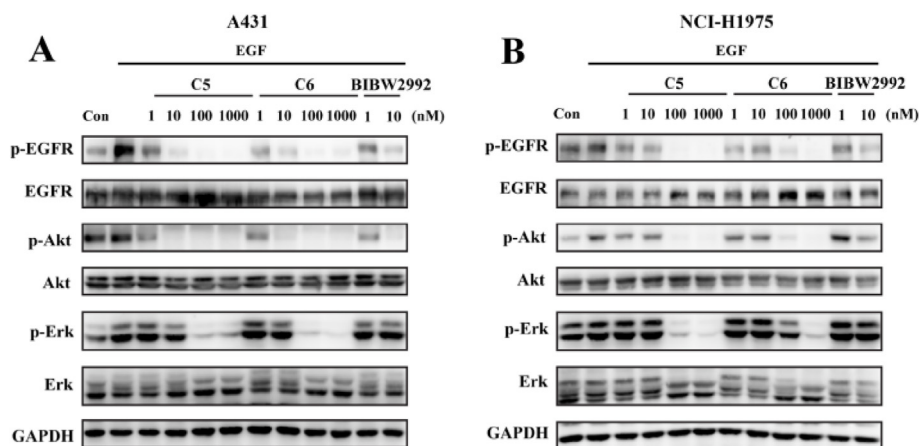


Fig. 3. Inhibitory effects of **C5** and **C6** on EGFR signaling across tumor cells carrying mutant/wild type EGFR, A431 (A) or NCI-H1975 (B) with the demonstrated concentrations of **C5**, **C6**, or BIBW2992 for 2 h, followed by stimulation for 15 min through EGF. Western blot analysis of total EGFR, p-EGFR, and downstream signalling proteins performed on cell lysates.

Table 4
Multi-kinase assay (IC₅₀, nM) of **C5**, **C6**, and BIBW2992 on HER2, HER4 and 11 other RTKs.

Kinase	C5	C6	BIBW2992
HER2	3.5 ± 0.8	75.1 ± 8.5	12.5 ± 0.9
HER4	1.6 ± 0.6	2.0 ± 0.0	7.2 ± 2.5
Src, VEGFR2, EPH-A2, IGF1R, ABL, FGFR1, Flt-1, c-Kit, PDGFR-α, PDGFR-β and RET	>10000	>10000	>10000

used to stimulate the H1975 cells for 24, 48, or 72 h. As depicted in Fig. 6A, these two compounds showed greater apoptosis induction effect than that of the control group in both early (lower right) and late apoptosis (upper right). The H1975 cells underwent apoptosis starting from 0.1 μM/24 h, and the effects were enhanced with increase in concentration and time. Thus, it was evident that these two compounds could induce cell apoptosis in a dose-dependent manner. The apoptosis ratios of **C5/C6** at different concentrations were 25.9/13.8% (0.1 μM), 40.3/37.8% (1 μM), and 66.1/50.7% (10 μM) measured at different concentrations at 72 h.

For further confirming the apoptotic mechanism, **C5** and **C6** were tested to detect caspase-triggering using western blot assay. Poly ADP-ribose polymerase (PARP) is a major substrate of the activated caspases, cleavage of which is one of the indicators of caspase-dependent apoptosis [27]. Our results revealed that the level of caspase-3 was increased and PARP was cleaved in a dose-dependent manner after treatment with **C5** and **C6** at concentrations of 0.1, 1, or 10 μM (Fig. 6B), especially when the time was increased to 72 h. These findings confirmed the results from flow cytometry analysis that **C5** and **C6** could induce caspase-dependent apoptosis.

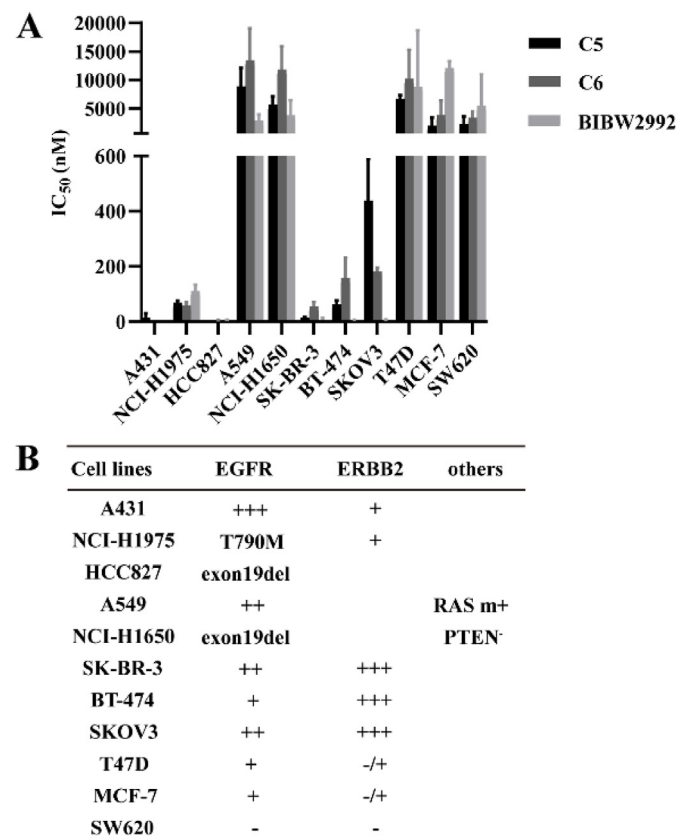


Fig. 4. *In vitro* antiproliferative effects (A) of **C5** and **C6**. The inserted table (B) shows the EGFR, HER2 (ERBB2), or other genes status of different cells. Growth inhibitory activity of **C5**, **C6**, or BIBW2992 was assessed by implementing the SRB colorimetric assessment. IC₅₀ Values are presented as the mean ± SD from three independent assessments.

2.6. Cell cycle analysis

To further investigate the pattern of how **C5** and **C6** inhibited the growth of cancer cells, cell cycle analysis was performed, as shown in Fig. 7. Compounds **C5**, **C6**, and BIBW2992 were delivered to H1975 and SKOV3 cells at a concentration of 1 μM. These two compounds arrested the progression of the cell cycle to the G1 phase, which is comparable to the effect of BIBW2992 on these two cell lines. The percentage of cells in the S phase in these three groups decreased in comparison with the control group. At the same time, the percentage of cells in the G2/M phase in these three groups decreased slightly in the H1975 cells; however, the situation of the SKOV3 cells was different. Overall, **C5** and **C6** arrested the cell cycle mainly in the G1 phase in the two kinds of cells as efficiently as BIBW2992.

2.7. Confirmation of the interaction mechanism

Compounds **C5** and **C6** were designed to be irreversible and reversible inhibitors, respectively. To verify the type of inhibition, the reversibility of EGFR binding was ascertained by employing a dilution approach using kinetic assessments. In this method, an amount of receptor 100 times that typically employed in a reaction was preincubated for 30 min with a concentration of **C5** or **C6** 100-fold higher than the IC₅₀ value or with the vehicle that served as the control. After incubation, the mixture of inhibitor/enzyme was diluted 100-fold, for instance to the normal reaction circumstances, reaction buffer plus substrate and ATP were added, and the receptor kinase activity was evaluated constantly. Generally, the dissociation of reversible inhibitor occurs rapidly, which provides instant recovery of enzymatic activity, whilst an irreversible inhibitor prevents recovery of the enzymatic activity [23]. BIBW2992 and erlotinib belong to irreversible and reversible EGFR inhibitors, respectively. As shown in Fig. 8, **C5** was proved to be an irreversible inhibitor (Fig. 8A), similar to the irreversible EGFR inhibitor BIBW2992 (Fig. 8C). On the other hand, the mode of action of **C6** (Fig. 8B) was similar to that of the reversible EGFR inhibitor erlotinib (Fig. 8D); hence, **C6** was a reversible inhibitor.

Based on the established interaction mechanism of **C5** and **C6** with EGFR, molecular docking investigations were conducted to explore the binding mode using the Glide module of the Schrodinger-2018-1 package version program. Crystal structures of EGFR T790M (Fig. 9C, PDB code: 4G5P) and WT (Fig. 9F, PDB code: 4G5J) in complex with BIBW2992 were used to make comparison with our docking results (Fig. 9A, B, D, and E). As depicted, the α,β-unsaturated carbonyl group of **C5** could covalently bind to the thiol group of Cys797 in EGFR T790M (Fig. 9A) and WT (Fig. 9D) to form irreversible interactions, which were the same as the irreversible binding manner of BIBW2992 (Fig. 9C and F). Conversely, **C6** could bind to EGFR T790M (Fig. 9B) and WT (Fig. 9E) in noncovalent manner. Especially for the binding interaction of **C6** with EGFR T790M, the three hydrogen bonds and one halogen bond may responsible for the potent inhibition.

Therefore, compound **C5** took an irreversible form in the interaction with EGFR. Compound **C6** could be defined as a reversible pan-HER inhibitor. To the best of our knowledge, compound **C6** is

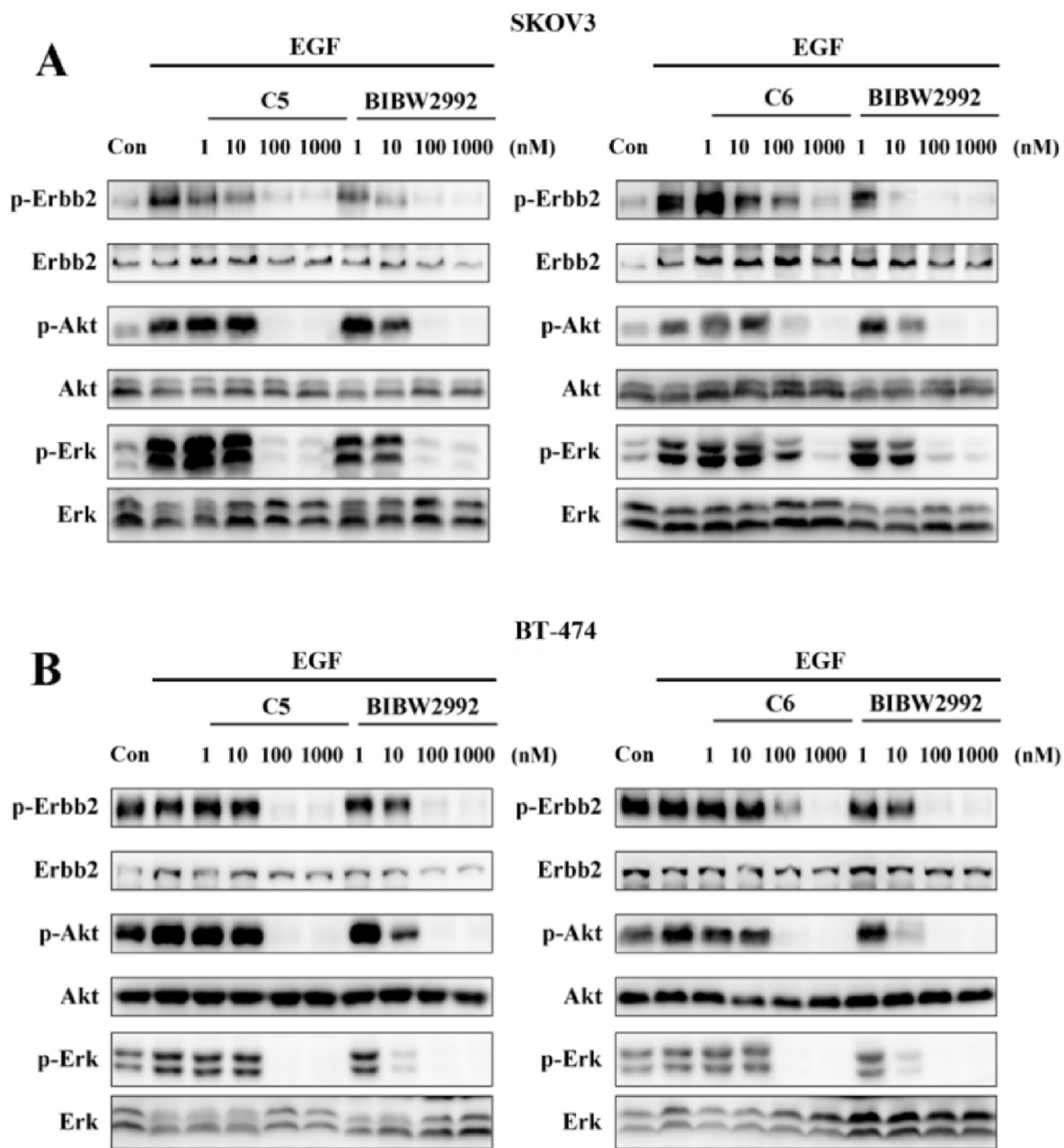


Fig. 5. Inhibitory effects of **C5** and **C6** on HER2 (ErbB2) signaling in SKOV3 (A) and BT-474 cells (B). SKOV3 (A) or BT-474 cells (B) were treated with **C5**, **C6**, or BIBW2992 for 2 h, followed by stimulation for 15 min through EGF. Western blotting of p-HER2, total HER2, and downstream signaling proteins performed on cell lysates.

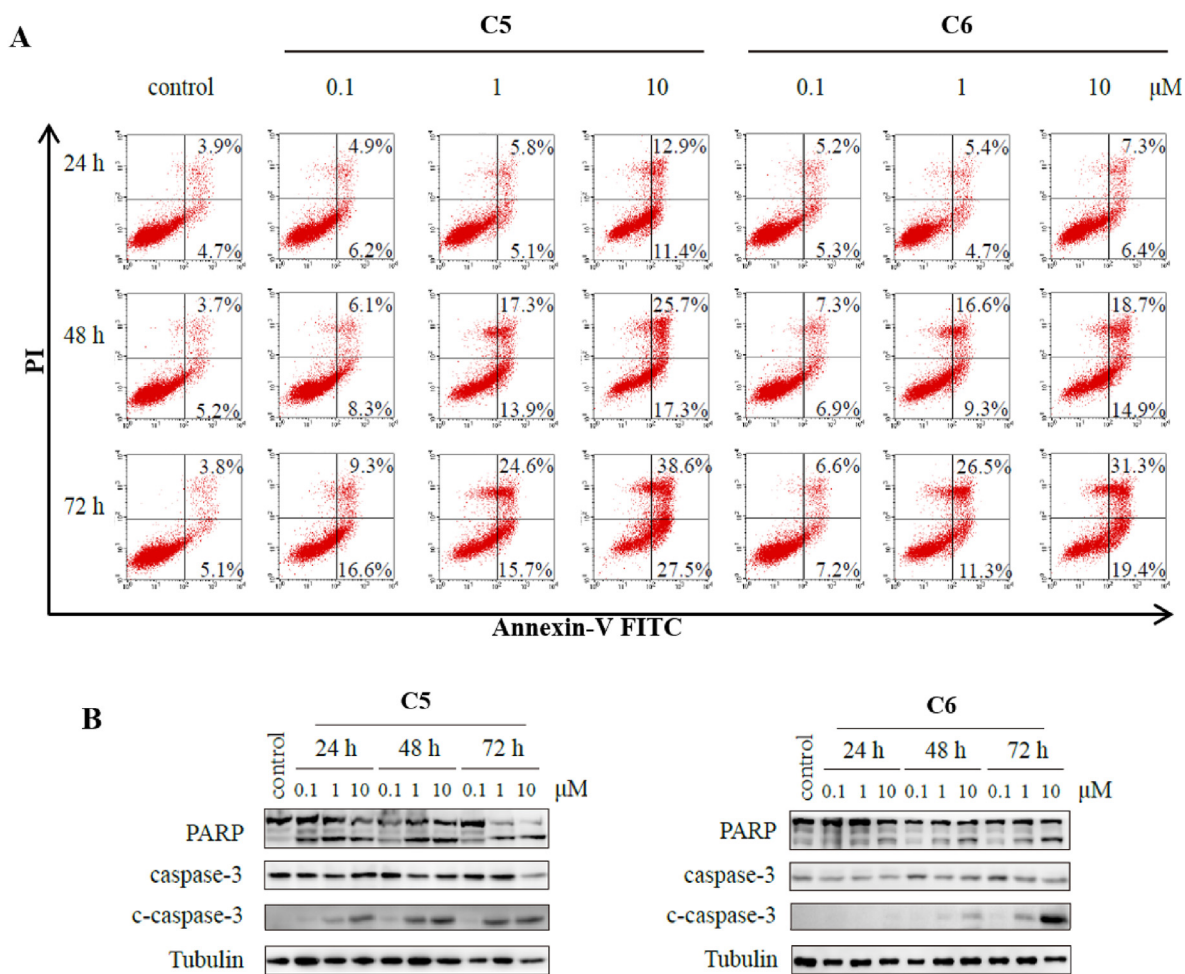


Fig. 6. H1975 cells were treated with **C5** and **C6** for 24/48/72 h, and subsequently subjected through Annexin V/PI stain-testing (**A**) and Western blotting (**B**). (**A**) The percentage of cells undergoing apoptosis was defined as the sum of early-apoptotic, late-apoptotic, and death cells; Upper right: late-apoptotic cells labeled with PI and Annexin-V; Lower left: living cells; Lower right: early apoptotic cells labeled with Annexin-V, but not with PI. (**B**) Activation of caspase-3 and PARP, and caspase-3/PARP proteomic expression detected by Western blotting.

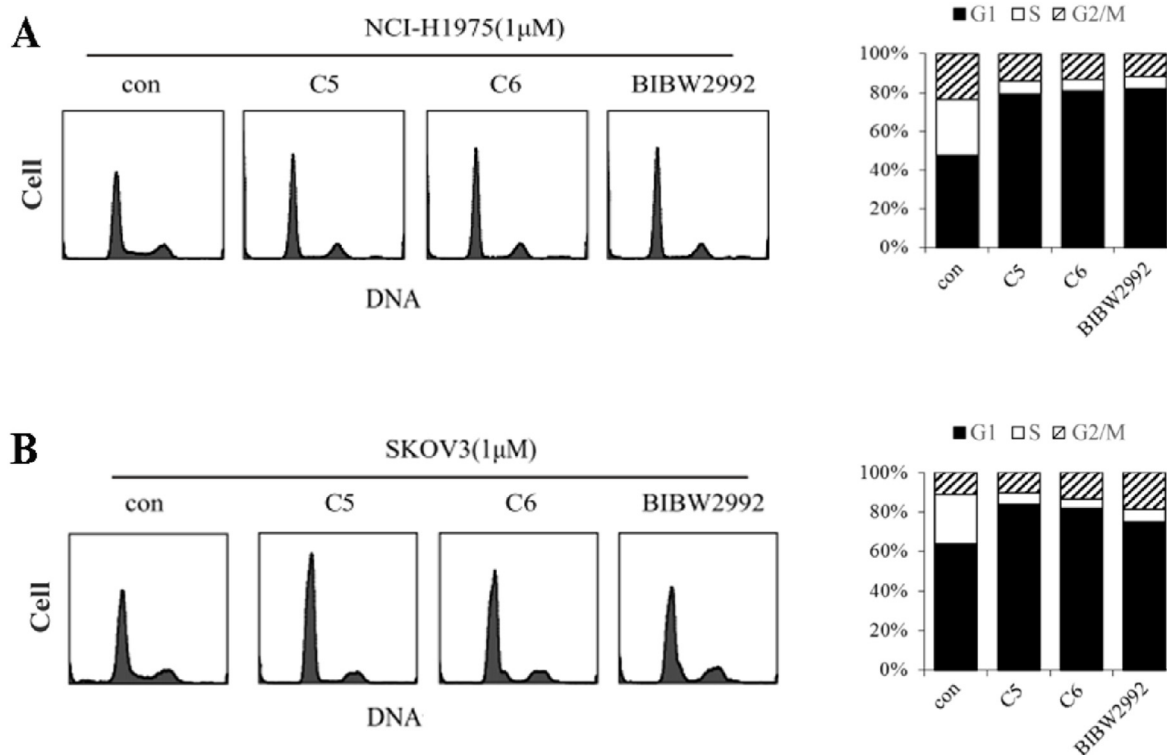


Fig. 7. Effects of **C5** and **C6** on cell cycle progression. Distributions of cell cycle after H1975 (**A**) or SKOV3 (**B**) treated with dimethyl sulfoxide (DMSO) control, **C5**, **C6**, or BIBW2992. Cell cycle distribution of different treatment groups is presented by quantitative analysis.

the first reported high-strength reversible pan-HER inhibitor with the capability of inhibiting HER1s (such as EGFR T790M/L858R and WT), HER2, and HER4. This finding is considered as a breakthrough in the drug discovery of reversible pan-HER inhibitors.

2.8. Antitumor efficacy *in vivo*

The antitumor efficacy *in vivo* of compound **C5** (Fig. 10A) and **C6** (Fig. 10B) was tested in EGFR WT high expression cells A431 xenograft mouse model. The right flanks of BALB/c nude mice were subcutaneously injected with A431 cells (5×10^6). When the volume of the tumor reached around 80–120 mm³, two groups of mice were treated with compound **C5** (20 mg/kg, oral or 80 mg/kg, oral) or **C6** (20 mg/kg, oral or 80 mg/kg, oral) ($n = 7$) once daily (QD) for 21 days. The group of negative control was also recruited, which was given only the vehicle. The results demonstrated that these two compounds resulted in definite tumor growth inhibition (20 mg/kg or 80 mg/kg) compared with the vehicle-treated controls. It is noteworthy that no obvious changes in body weight were observed in any of the treatment groups. The results from western blot confirmed that these two compounds could thwart EGFR/Akt/ERK phosphorylating events within the tumor tissues of the nude mice. Therefore, compounds **C5** and **C6** could be considered as promising antitumor agents.

3. Conclusions

In summary, a total of 27 target compounds based on *N*-(ring structure fused phenyl)quinazoline-4-amine were designed, synthesized, and biologically evaluated *in vitro* and *in vivo*. Compound **C5** with the molecular skeleton of *N*-(3-bromo-1*H*-indol-5-yl)-quinazolin-4-amine was confirmed to act as an irreversible pan-

HER inhibitor. To our surprise, compound **C6** with the same skeleton was found to be a high-strength reversible pan-HER inhibitor capable of inhibiting HER1s (such as T790M/L858R and WT), HER2, and HER4, which could be viewed as a breakthrough in the development of pan-HER inhibitors. Overall, compounds **C5** and **C6** are promising antitumor agents, and the corresponding molecular skeleton can be used to design both reversible and irreversible pan-HER inhibitors for the development of antitumor drugs.

4. Experimental

4.1. General methods of chemistry

All solvents and chemicals were purchased from relevant companies (Sigma-Aldrich, Aladdin, Alfa Aesar, or J&K Scientific) and used without additional refinement unless stated otherwise. Column chromatography was performed using silica gel (Qingdao Marine Chemical Factory™, China), and thin-layer chromatography (TLC) was also performed using silica gel (GF254, Qingdao Haiyang™ Chemical Co., Ltd, China). Electron-spray ionization mass spectrometry (ESI-MS) was performed through Bruker Esquire™ 3000t spectrometer. ¹³C NMR/¹H NMR spectra were registered over the Bruker™ 500/600 MHz instrument. All recorded spectra were referenced to the solvent signal or TMS. With the aid of a Fisher-Johns melting apparatus, the uncorrected melting points were determined. Analytical high-performance liquid chromatography (HPLC) was performed using the Agilent™ 1260® LC/Inertex-C18 column, and the compound elution quality (purity) was found to be >95%. Owing to space constraints, general preparatory methods and data related to chemical structures of the compounds/intermediates have been moved to the [Supporting Information file](#).

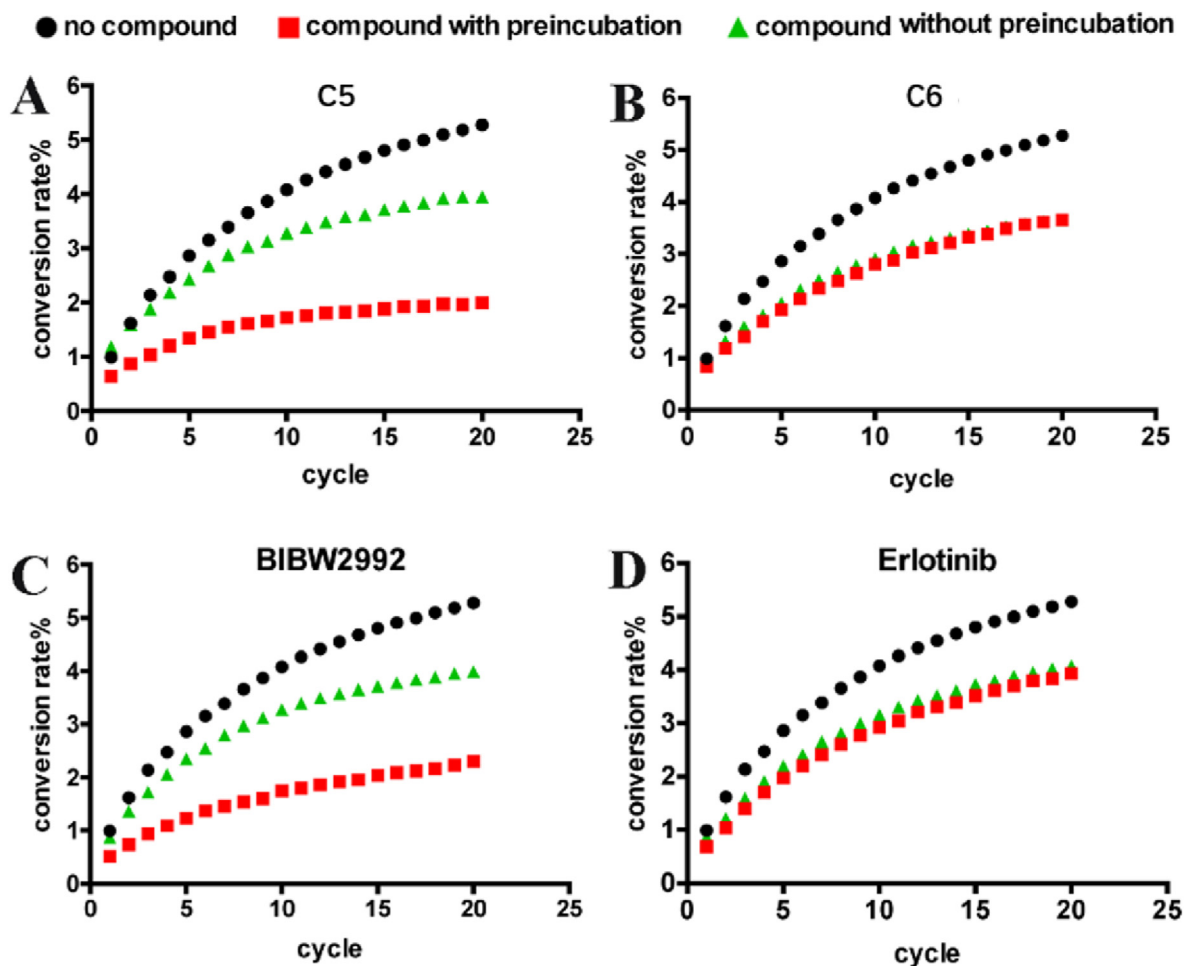


Fig. 8. Target-inhibition reversibility analyses of C5 and C6. Mobility-Shift assay was performed to evaluate the inhibition reversibility of C5 (A), C6 (B), BIBW2992 (C), and erlotinib (D) against EGFR kinases. EGFR kinases were preincubated with excess compounds for 30 min, and then interacted with the reaction solution containing a substrate. Kinetic analyses of EGFR-substrate reaction performed using the EZ Caliper Reader.

4.2. Kinase activity assay

EGFR WT (#14–531M), EGFR T790M (#14–725), EGFR L858R/T790M (#14–721MM), HER2 (#14–939M), and HER4 (#14–569M) proteins were procured from Eurofins (Brussels, Belgium). Kinase activity was assessed using ELISA. Poly-(Glu, Tyr; 4:1), amounting to 20 μ M, was pre-permeated on 96-well ELISA plates (substrate). Functioning kinases were incubated together with the investigated substances in 1 \times reaction buffer (50 mM HEPES pH 7.4, 20 mM MgCl₂, 0.2 mM Na₃VO₄, 0.1 mM MnCl₂, and 1 mM DTT) containing 5 μ M ATP (37 °C/60 min). The plate contents were then rinsed with phosphate buffered saline (PBS), followed by incubation with anti-phosphotyrosine (PY99) antibody (Santa Cruz Biotechnology™, USA). This step was succeeded by reincubation with horseradish peroxidase-conjugated secondary antibody. The plate contents were visualized using o-phenylenediamine (OPD), and the absorbance was determined using a multiwall spectrophotometer (VERSAmax®, Molecular Devices™, USA) at 490 nm [26].

4.3. Cell culture

A431, NCI-H1975, HCC827, A549, NCI-1650, SK-BR-3, BT-474, SKOV3, T47D, MCF-7, and NIH3T3, as well as SW620 cultures, were acquired from American Type Culture Collection (ATCC). NIH3T3 cultures that overexpressed 19D/T790M, EGFR L858R,

T790M/L858R, and insNPG mutant were fabricated and maintained in the laboratory. The cells were preserved in appropriate culture media as the supplier's instructions, and all cell lines were verified using a short tandem repeat (STR) assessment.

4.4. Antiproliferative assay

The antiproliferation functions of the agents were appraised using sulforhodamine B (SRB®; Sigma™, USA) colorimetric assessment. The cells were seeded in 96-well plates during the night hours and then processed (three days) with dimethyl sulfoxide (DMSO) control or serially diluted assay substances. Subsequently, SRB assessment was performed according to standardized guidelines already explained [28]. The IC₅₀ values were determined using the four-parameter logit method. The achieved outcomes reflected mean \pm standard deviation (SD) of three separate measurements.

4.5. Western blot assessment

The cells were collected and treated with sodium dodecyl sulfate (SDS) lytic buffer, followed by boiling (20 min). The specimens for cell lysis were subjected to SDS-polyacrylamide gel electrophoresis (PAGE), transferred to nitrocellulose-membranes, blocked for 1 h at ambient temperature with 5% milk-Tris-buffered saline

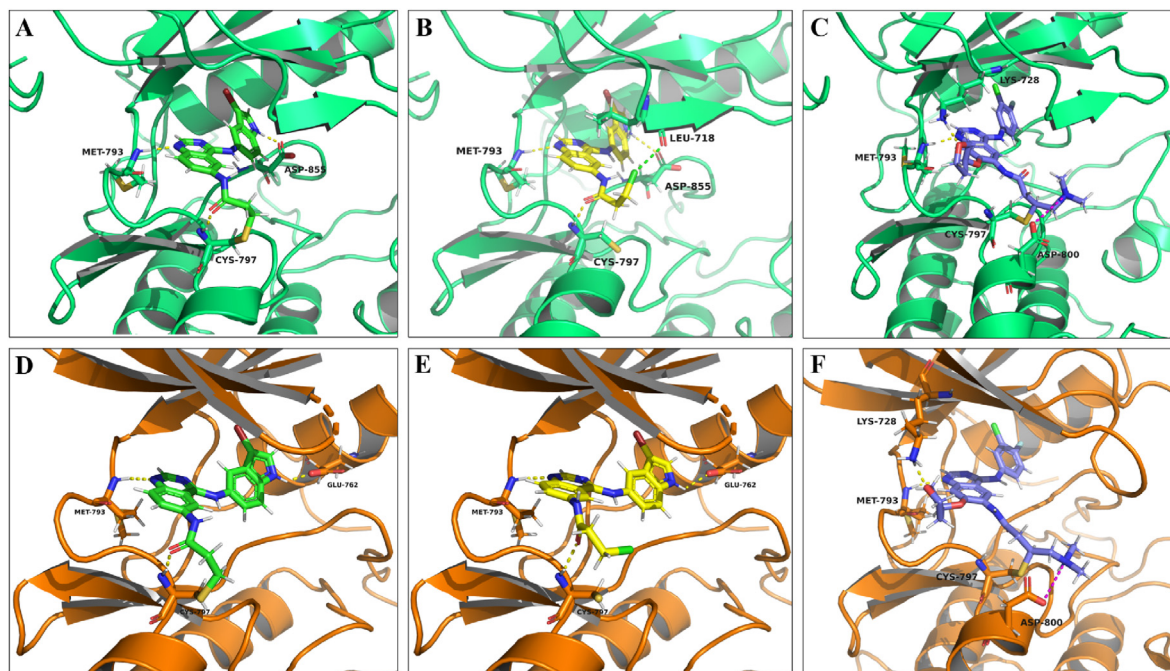


Fig. 9. Docking results of C5 and C6 with EGFR T790M (Fig. 9A and B) and WT (Fig. 9D and E), crystal structures of EGFR T790M (Fig. 9C) and WT (Fig. 9F) in complex with BIBW2992. EGFR T790M (PDB code: 4G5P) is displayed by green cartoon. EGFR WT (PDB code: 4G5J) is displayed by orange cartoon. C5 is displayed by green multicolour sticks. C6 is displayed by yellow multicolour sticks. BIBW2992 is displayed by blue multicolour sticks. The H-bonding interactions are displayed with dashed yellow lines. The halogen bond is displayed with dashed wine-red lines. The salt-bridge interactions are displayed with dashed green lines.

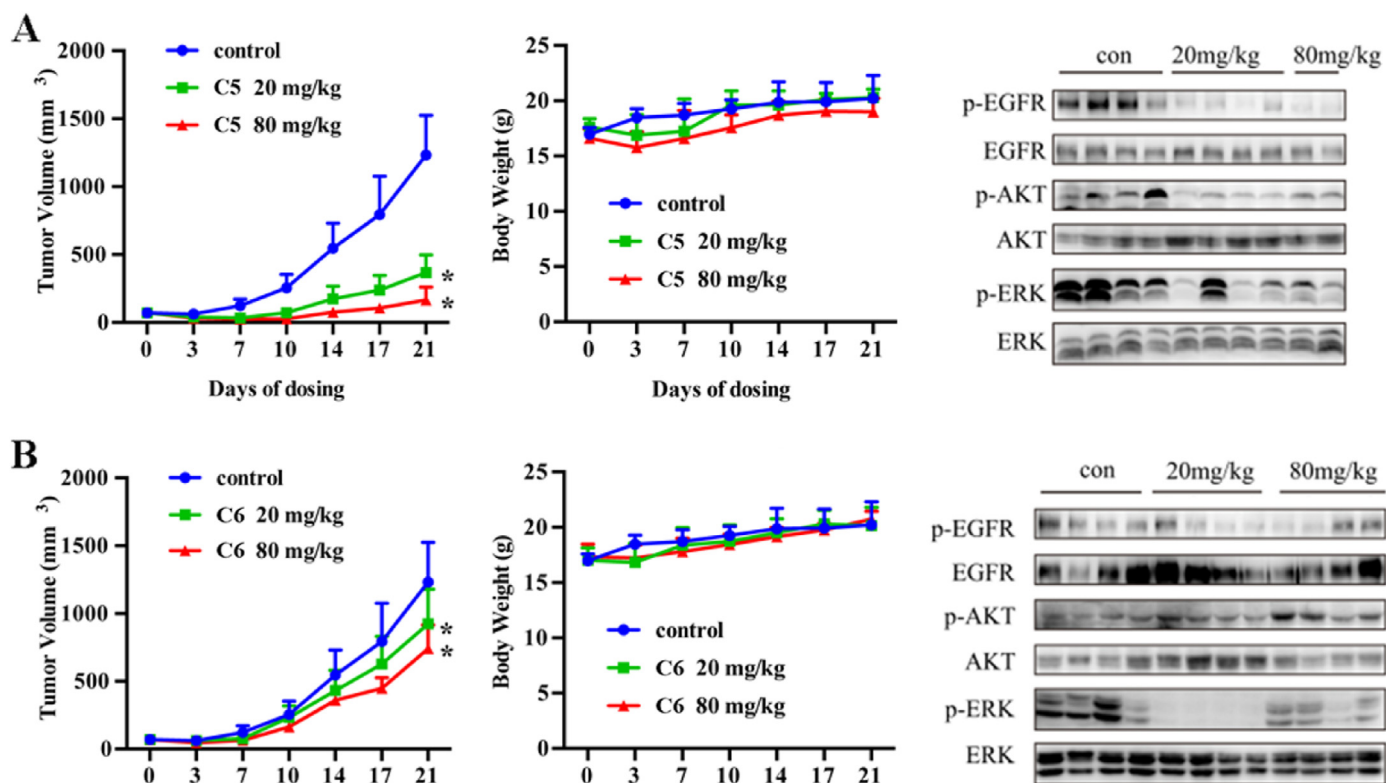


Fig. 10. *In vivo* antitumor effects of C5 (A) and C6 (B) on A431 (EGFR WT) xenograft models. Mice bearing A431 xenograft tumors were treated with vehicle control, C5 (20 mg/kg, oral or 80 mg/kg, oral) or C6 (20 mg/kg, oral or 80 mg/kg, oral) (n = 7). Every 2–3 days, the tumor volumes and body weight were measured; the results are presented as mean ± SD. *p < 0.05 vs control group. After treatment with the indicated compounds for 21 days, the inhibitory effects of C5 (A) or C6 (B) on EGFR signaling in A431 xenograft tumors were determined by Western blotting (2 or 4 mice randomly selected from each group).

with Tween (TBST), and blotted using primary antibodies (4 °C/overnight). Following triple-rinse steps using TBST, all membranes were exposed to horseradish peroxidase (HRP)-conjugated secondary antibodies (Jackson, #111-035-003) for 1 h. Western blot assessment was then performed using standard processes. Tumor tissues were lysed with radioimmunoprecipitation assay (RIPA) lysis buffer, and the concentrations of the proteins were ascertained using the standard Bradford assessment for normalizing the specimens. For blotting, equivalent proteomic content was subjected to SDS-PAGE.

4.6. Chemicals and antibodies

BIBW2992 (#S1011) and erlotinib (#S7786) were purchased from Selleck. 1° antibodies against phospho-EGFR (Tyr1068; #3777), EGFR (#4267), phospho-HER2/ErbB2 (Tyr1221/1222; #2243), HER2/ErbB2(#4290), phospho-HER4/ErbB4 (Tyr1284; #4757), HER4/ErbB4 (#4795), phospho-AKT (Ser473; #4060), pan-AKT (#4691), phospho-ERK (T202/Y204; #4370), and ERK1/2 (#4695) were all purchased from the Cell Signaling Technologies.

4.7. Xenograft mouse model

The A431 cells (5×10^6) were subcutaneously injected on the right-hand side for BALB/c nude murines. The tumor-bearing mice were randomized into vehicle and treatment groups when the average tumor volume reached 80–120 mm³. Tumor growth was examined twice per week, and tumor volume was measured with a caliper using the formula $(\text{length} \times \text{width}^2)/2$. All lines of action relevant to animal care, handling, and processing were performed as per the protocols laid down by the Institutional Animal Care and Use Committee in compliance with the Association for Assessment and Accreditation of Laboratory Animal Care.

Declaration of competing interest

The authors declare that they have no known competing financial interests or personal relationships that could have appeared to influence the work reported in this paper.

Acknowledgments

This work was supported by the National Key Research Project (2017YFA0506000 to Guang Liang), National Natural Science Foundation of China (81930108 to Guang Liang, 81903638 to Tao Zhang), Wenzhou Science and Technology Key Project (2018ZY009 to Guang Liang), and "Personalized Medicines-Molecular Signature-based Drug Discovery and Development", Strategic Priority Research Program of the Chinese Academy of Sciences (XDA12020112 to Hua Xie).

Appendix A. Supplementary data

Supplementary data to this article can be found online at <https://doi.org/10.1016/j.ejmech.2022.114249>.

References

- [1] J. Schlessinger, Cell signaling by receptor tyrosine kinases, *Cell* 103 (2000) 211–225.
- [2] J. Lategahn, M. Keul, D. Rauh, Lessons to be learned: the molecular basis of kinase-targeted therapies and drug resistance in non-small cell lung cancer, *Angew. Chem.* 57 (2018) 2307–2313.
- [3] X. Wang, K. Batty, P. Crowe, D. Goldstein, J. Yang, The potential of panHER inhibition in cancer, *Front. Oncol.* 5 (2015) 2.
- [4] R. Roskoski, Small molecule inhibitors targeting the EGFR/ErbB family of protein-tyrosine kinases in human cancers, *Pharmacol. Res.* 139 (2019)

- 395–411.
- [5] E. Cocco, F. Javier Carmona, P. Razavi, H. Won, Y. Cai, V. Rossi, C. Chan, J. Cownie, J. Soong, E. Toska, S. Shifman, I. Sarotto, P. Savas, M. Wick, K. Papadopoulos, A. Moriarty, R. Cutler, F. Avogadri-Connors, A. Lalani, R. Bryce, S. Chandrapaty, D. Hyman, D. Solit, V. Boni, S. Loi, J. Baselga, M. Berger, F. Montemurro, M. Scaltriti, Neratinib is effective in breast tumors bearing both amplification and mutation of ERBB2 (HER2), *Sci. Signal.* (2018) 11.
- [6] J. Meng, X. Liu, S. Ma, H. Zhang, S. Yu, Y. Zhang, M. Chen, X. Zhu, Y. Liu, L. Yi, X. Ding, X. Chen, L. Miao, D. Zhong, Metabolism and disposition of pyrotinib in healthy male volunteers: covalent binding with human plasma protein, *Acta Pharmacol. Sin.* 40 (2019) 980–988.
- [7] H. Udagawa, S. Hasako, A. Ohashi, R. Fujioka, Y. Hakozaiki, M. Shibuya, N. Abe, T. Komori, T. Haruma, M. Terasaka, R. Fujita, A. Hashimoto, K. Funabashi, H. Yasuda, K. Miyadera, K. Goto, D. Costa, S. Kobayashi, EGFR-TKIs with a broad spectrum of preclinical activity against clinically relevant mutations, *Mol. Cancer Res.* MCR 17 (2019) 2233–2243.
- [8] G. Kaushik, P. Seshacharyulu, S. Rauth, P. Nallasamy, S. Rachagani, R. Nimmakayala, R. Vengoji, K. Mallya, R. Chirravuri-Venkata, A. Singh, J. Foster, Q. Ly, L. Smith, S. Lele, M. Malafa, M. Jain, M. Ponnusamy, S. Batra, Selective inhibition of stemness through EGFR/FOXO2/SOX9 axis reduces pancreatic cancer metastasis, *Oncogene* 40 (2021) 848–862.
- [9] Y. Zhang, Z. Zhang, X. Huang, S. Kang, G. Chen, M. Wu, S. Miao, Y. Huang, H. Zhao, L. Zhang, Therapeutic efficacy comparison of 5 major EGFR-TKIs in advanced EGFR-positive non-small-cell lung cancer: a network meta-analysis based on head-to-head trials, *Clin. Lung Cancer* 18 (2017) e333–e340.
- [10] R. Shah, J. Lester, Tyrosine kinase inhibitors for the treatment of EGFR mutation-positive non-small-cell lung cancer: a clash of the generations, *Clin. Lung Cancer* 21 (2020) e216–e228.
- [11] X. Yu, X. Zhao, J. Zhang, Y. Li, P. Sheng, C. Ma, L. Zhang, X. Hao, X. Zheng, Y. Xing, H. Qiao, L. Qu, D. Zhu, Dacomitinib, a new pan-EGFR inhibitor, is effective in attenuating pulmonary vascular remodeling and pulmonary hypertension, *Eur. J. Pharmacol.* 850 (2019) 97–108.
- [12] B. Dahal, T. Cornitescu, A. Tretny, S. Pullamsetti, D. Kosanovic, R. Dumitrascu, H. Ghofrani, N. Weissmann, R. Voswinkel, G. Banat, W. Seeger, F. Grimminger, R. Schermuly, Role of epidermal growth factor inhibition in experimental pulmonary hypertension, *Am. J. Respir. Crit. Care Med.* 181 (2010) 158–167.
- [13] J. Zhang, J. Cao, J. Li, Y. Zhang, Z. Chen, W. Peng, S. Sun, N. Zhao, J. Wang, D. Zhong, X. Zhang, J. Zhang, A phase I study of AST1306, a novel irreversible EGFR and HER2 kinase inhibitor, in patients with advanced solid tumors, *J. Hematol. Oncol.* 7 (2014) 22.
- [14] R. Phillips, Targeting the hypoxic fraction of tumours using hypoxia-activated prodrugs, *Cancer Chemother. Pharmacol.* 77 (2016) 441–457.
- [15] J. Kim, E. Lee, K. Park, H. Jung, W. Park, K. Lee, J. Sohn, K. Lee, K. Jung, J. Kim, K. Lee, S. Im, Y. Park, Molecular alterations and poziotinib efficacy, a pan-HER inhibitor, in human epidermal growth factor receptor 2 (HER2)-positive breast cancers: combined exploratory biomarker analysis from a phase II clinical trial of poziotinib for refractory HER2-positive breast cancer patients, *Int. J. Cancer* 145 (2019) 1669–1678.
- [16] V. von Manstein, B. Groner, Tumor cell resistance against targeted therapeutics: the density of cultured glioma tumor cells enhances Stat3 activity and offers protection against the tyrosine kinase inhibitor canertinib, *MedChemComm* 8 (2017) 96–102.
- [17] C. Liu, P. Chu, C. Huang, J. Chen, H. Yang, W. Wang, K. Lau, C. Lee, T. Lan, T. Huang, P. Lin, M. Dai, L. Tseng, Valtinib downregulates HER/ERK signaling and induces apoptosis in triple negative breast cancer cells, *Cancers* 11 (2019).
- [18] Y. Kim, L. Bhatt, H. Ahn, Z. Yang, W. Lee, H. Nam, Suppressors for human epidermal growth factor receptor 2/4 (HER2/4): a new family of anti-toxoplasmic agents in ARPE-19 cells, *Kor. J. Parasitol.* 55 (2017) 491–503.
- [19] S. Johnston, M. Basik, R. Hegg, W. Lausoontornsiri, L. Grzeda, M. Clemons, L. Dreosti, H. Mann, M. Stuart, M. Cristofanilli, Inhibition of EGFR, HER2, and HER3 signaling with AZD8931 in combination with anastrozole as an anti-cancer approach: phase II randomized study in women with endocrine-therapy-naïve advanced breast cancer, *Breast Cancer Res. Treat.* 160 (2016) 91–99.
- [20] D. Das, J. Hong, Recent advancements of 4-aminoquinazoline derivatives as kinase inhibitors and their applications in medicinal chemistry, *Eur. J. Med. Chem.* 170 (2019) 55–72.
- [21] Y. Van Sebillie, R. Gibson, H. Wardill, J. Bowen, ErbB small molecule tyrosine kinase inhibitor (TKI) induced diarrhoea: chloride secretion as a mechanistic hypothesis, *Cancer Treat Rev.* 41 (2015) 646–652.
- [22] F. Solca, G. Dahl, A. Zoepfel, G. Bader, M. Sanderson, C. Klein, O. Kraemer, F. Himmelsbach, E. Haakma, G. Adolf, Target binding properties and cellular activity of afatinib (BIBW 2992), an irreversible ErbB family blocker, *J. Pharmacol. Exp. Therapeut.* 343 (2012) 342–350.
- [23] H. Xie, L. Lin, L. Tong, Y. Jiang, M. Zheng, Z. Chen, X. Jiang, X. Zhang, X. Ren, W. Qu, Y. Yang, H. Wan, Y. Chen, J. Zuo, H. Jiang, M. Geng, J. Ding, AST1306, a novel irreversible inhibitor of the epidermal growth factor receptor 1 and 2, exhibits antitumor activity both *in vitro* and *in vivo*, *PLoS One* 6 (2011), e21487.
- [24] J.Y. Lee, Y.S. Shin, J. Lee, S. Kwon, Y. Jin, M.S. Jang, S. Kim, J.H. Song, H.R. Kim, C.M. Park, Identification of 4-anilino-6-aminoquinazoline derivatives as potential MERS-CoV inhibitors, *Bioorg. Med. Chem. Lett* 30 (20) (2020) 127472.

- [25] B. Marvania, P. Lee, R. Chaniyara, H. Dong, S. Suman, R. Kakadiya, T. Chou, T. Lee, A. Shah, T. Su, Design, synthesis and antitumor evaluation of phenyl N-mustard-quinazoline conjugates, *Bioorg. Med. Chem.* 19 (2011) 1987–1998.
- [26] Y. Liu, Y. Wang, X. Lu, L. Tong, Y. Li, T. Zhang, Q. Xun, F. Feng, Y. Chen, Y. Su, Y. Shen, Y. Chen, M. Geng, K. Ding, Y. Li, H. Xie, J. Ding, Identification of compound D2923 as a novel anti-tumor agent targeting CSF1R, *Acta Pharmacol. Sin.* 39 (2018) 1768–1776.
- [27] Y. Li, W. Fan, Q. Gong, J. Tian, M. Zhou, Q. Li, L. Uwituze, Z. Zhang, R. Hong, R. Wang, Structure-based optimization of 3-phenyl-N-(2-(3-phenylureido)ethyl)thiophene-2-sulfonamide derivatives as selective mcl-1 inhibitors, *J. Med. Chem.* 64 (2021) 10260–10285.
- [28] Z. Chen, L. Tong, B. Tang, H. Liu, X. Wang, T. Zhang, X. Cao, Y. Chen, H. Li, X. Qian, Y. Xu, H. Xie, J. Ding, C11, a novel fibroblast growth factor receptor 1 (FGFR1) inhibitor, suppresses breast cancer metastasis and angiogenesis, *Acta Pharmacol. Sin.* 40 (2019) 823–832.